Radial Distribution of Spallogenic K, Ca, Ti, V and Mn Isotopes in Iron Meteorites

Mineo Imamura *, Masako Shima **, and Masatake Honda
The Institute for Solid State Physics, The University of Tokyo

Z. Naturforsch. **35a**, 267–279 (1980); received January 7, 1980

Dedicated to Professor H. Hintenberger on the occasion of his 70th birthday

Cosmic-ray-produced stable nuclides of Ca (mass number: 42, 43, 44 and 46), Ti (46, 47, 49 and 50), V (50), Cr (50, 53 and 54) and the long-lived nuclides, ^{40}K and ^{53}Mn were determined along the radial axes of the iron meteorites Grant and Treysa. Grant was extensively examined and the results compared with rare gas data. Although Treysa does not include enough samples to allow detailed analysis, the depth profile shows typical features for a small meteorite.

The results were compared with calculated profiles of ^{40}K, ^{49}Ti and ^{53}Mn using thick bombardment data. The approximate pre-atmospheric radii of Grant and Treysa were determined to be 30 cm and 14 cm, respectively. The effect of space erosion was also estimated by comparing the data of ^{49}Ti and radioactive ^{53}Mn in Grant and Treysa with the calculated patterns. It is suggested that space erosion of both meteorites is small ($\lesssim 0.8$ Å/y) during the cosmic-ray exposure of several hundred million years.

1. Introduction

The interaction of primary cosmic radiation with meteorites produces many secondary particles of various energies, causing very complex nuclear reactions and a variety of nuclear species to be produced. The distribution of these products in the meteorite is a function of the shielding depth, viz. it depends on the shape and size of the meteoroid as well as the depth of the sample in the body. The investigation of these depth dependences of cosmogenic nuclides is important to the understanding of histories of cosmic-rays, meteorites and lunar surface materials.

Since the first determination of ^{3}He in iron meteorites by Paneth et al. [1], a large number of spallogenic rare gas data as well as their radial distribution has been published [2–12]. On the other hand the data of cosmic-ray produced spallogenic stable nuclides other than rare gases are limited to certain nuclides [13–19]. There have been many studies on spallogenic radioactive nuclides, but only a little work [18] has been reported on depth profiles in the iron meteorites.

Among the spallogenic nuclides in iron meteorites, the production rate of rare-gas isotopes decreases with the depth of the sample, that is, production correlates almost linearly with the attenuation of high energy particles. Compared with rare gas isotopes, nuclides of mass number closer to target nuclides, such as ^{53}Mn, ^{54}Cr, ^{50}V, ^{50}Ti, etc., are produced in a large proportion by moderate energy secondaries. These nuclides give a maximum in the distribution patterns along the depth of samples [20, 21]. As is well known, the maximum positions in the distribution patterns of these spallogenic nuclides are almost inversely related to the mass differences between target and produced nuclides. Therefore, it would be ideal to study spallogenic nuclides in a wide range of mass differences from the main target nuclides. Further, it is also desirable to measure spallogenic stable and radioactive nuclides in the same sample because comparisons of stable nuclides and radioactive nuclides with various half-lives make it possible to estimate the erosion rate in space and ablation in air, as well as the constancy of cosmic rays.

In this paper, we report the distribution of cosmic-ray-produced isotopes of Mn, Cr, V, Ca and K including ^{53}Mn ($T_{1/2} = 3.7 \times 10^{6}$ y) [22] and ^{40}K ($T_{1/2} = 1.28 \times 10^{9}$ y) [23, 24] in two iron meteorites, Grant and Treysa. Since, all the spallogenic nuclides in iron meteorites are predominantly produced from Fe and Ni, the analysis of the data is much less complex than in the case of stone mete-

* Present Address: Institute for Nuclear Study, The University of Tokyo, Midori-cho, Tanashi, Tokyo, 188, Japan.
** Present Address: National Science Museum, Ueno-Park, Taito-ku, Tokyo, 110, Japan.

Reprint requests to Dr. Masako Shima, National Science Museum, Ueno-Park, Taito-ku, 110, Japan.

0340-4811 / 80 / 0300-0267 $ 01.00/0. — Please order a reprint rather than making your own copy.

Dieses Werk wurde im Jahr 2013 vom Verlag Zeitschrift für Naturforschung in Zusammenarbeit mit der Max-Planck-Gesellschaft zur Förderung der Wissenschaften e.V. digitalisiert und unter folgender Lizenz veröffentlicht: Creative Commons Namensnennung-Keine Bearbeitung 3.0 Deutschland Lizenz.

This work has been digitalized and published in 2013 by Verlag Zeitschrift für Naturforschung in cooperation with the Max Planck Society for the Advancement of Science under a Creative Commons Attribution-NoDerivs 3.0 Germany License.

Zum 01.01.2015 ist eine Anpassung der Lizenzbedingungen (Entfall der Creative Commons Lizenzbedingung „Keine Bearbeitung") beabsichtigt, um eine Nachnutzung auch im Rahmen zukünftiger wissenschaftlicher Nutzungsformen zu ermöglichen.

On 01.01.2015 it is planned to change the License Conditions (the removal of the Creative Commons License condition "no derivative works"). This is to allow reuse in the area of future scientific usage.

orites. Grant, a medium-sized iron meteorite with recovered weight 530 kg, was chosen because a considerable number of detailed rare gas data are available [4, 9] and comparison with other data is possible. Treysa has not been investigated in detail, but it is an interesting object due to its smaller size with recovered weight 63.3 kg. The experimental data are compared with model calculations and discussed in connection with the pre-atmospheric size of meteorites, space erosion and the constancy of the cosmic-rays intensity.

2. Experimental

2.1. Samples

Sample locations in the plane cut out from the meteorites are shown in Figures 1 and 2. The planes are supposed to pass near the center of the meteorites based on rare gas distributions [4, 9]. The samples from Grant are from the plane investigated by Hoffman and Nier [4], Fireman [7], and Signer and Nier [9] for depth profile measurements of rare gases.

About lg chunks of each sample location were cut from Grant and Treysa with a steel fretsaw or a circular rubber saw. The surfaces of the specimens were etched and washed successively with 6 N HCl, 5 N HNO_3, water and ethanol or acetone. The absence of inclusions such as troilite and schreibersite was checked in the course of these treatments.

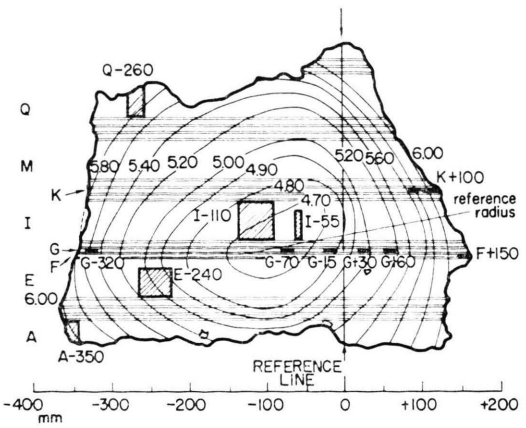

Fig. 1. Location of Grant samples used in this work. For example, "A-350" indicates that the specimen was taken from Bar A and at − 350 mm (at the center of the specimen) from the reference line, Contour lines shown in the figure are taken from the study of ^{3}He distribution by Hoffman and Nier [7]. The unit of the ^{3}He content is 10^{-6} ccSTP/g.

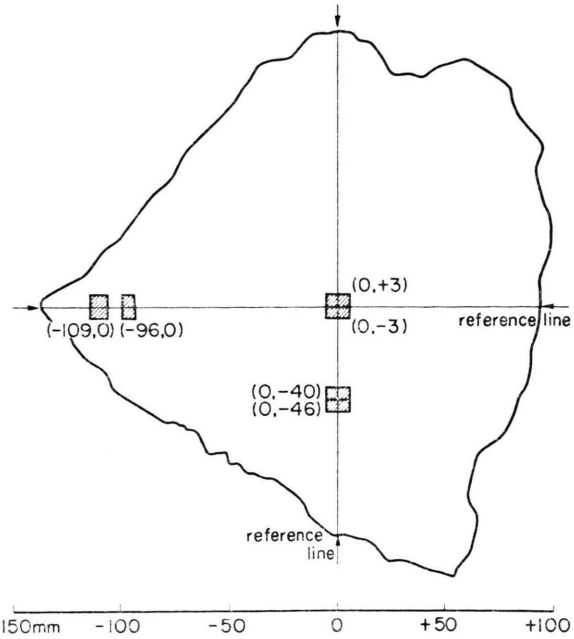

Fig. 2. Sample location of Treysa iron meteorite specimens used in this work. Location is shown as (x, y) coordinates.

2.2. Chemical Procedure

The sample was dissolved in a minimum amount of aqua regia. For the isotope dilution analyses, appropiate amounts of mixed spike solution containing ^{39}K-, ^{42}Ca-, and ^{46}Ti-enriched isotopes and V and Mn of terrestrial isotopic composition were added to the solution at the beginning of the dissolution process. Because of the complex chemical behaviour of Cr in the solution, another chunk was taken for Cr extraction and a ^{50}Cr-enriched spike was added to the sample.

All acids, ammonia and organic solvents used were purified by isopiestic- [25] or distillation methods under normal or reduced pressures. Chemical treatments were performed in a dust-free chamber positively pressurized by clean N_2. In most cases, teflon or quartz vessels were used. The detailed chemical procedures have already been described in our previous papers [14 – 16], and are schematically summarized in Figure 3.

2.3. Mass Spectrometry

The isotopic ratios of K, Ca, Ti, V and Cr were measured by a surface ionization source mass

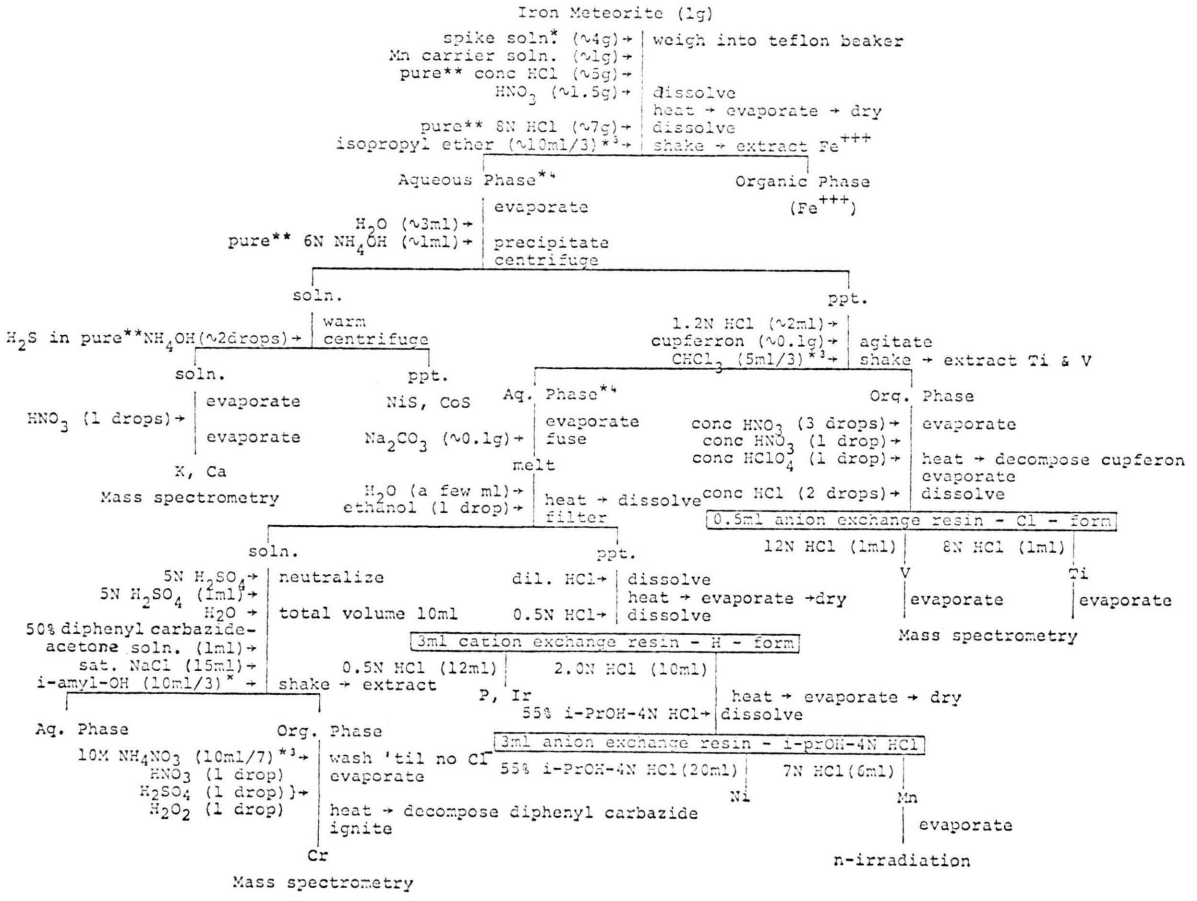

Fig. 3. Schematic diagram for the chemical separations of K, Ca, Ti, V, Cr and Mn from each other and from the target materials Fe, Ni and Co.

* Spike mixture solutions containing $\sim 1\,\mu g$ ^{39}K-, $\sim 0.1\,\mu g$ ^{42}Ca- and $\sim 0.01\,\mu g$ ^{46}Ti-enriched isotopes and $\sim 0.1\,\mu g$ V per 1 g solution. About 0.3 mg Mn/g carrier solution was prepared separately. Concentrations of all spikes and carrier were determined gravimetrically and/or by reverse isotope dilution analyses.

** Purified by isopiestic method. Other acids and organic solvents were purified by double distillation.

*3 "(∼ 10 ml/3)" expresses that extraction was repeated 3 times using total volume ∼ 10 ml of organic solvent, that is, in each extraction about 3.3 ml of organic solvent were used.

*4 When Cr was extracted separately for a different specimen, the aqueous phases from the Fe extraction by isopropyl ether were treated in the same way as described after this step.

spectrometer equipped with an electron multiplier, followed by a D.C. amplifier and a recording system. A digital voltmeter connected with a printer were used as well as a pen recorder.

The K and Cr were measured using a single filament ion source but Ti and V were measured with triple-filament techniques. Depending on the sample sizes, Ca was measured with both techniques. Details of the experimental procedure have been described elsewhere [14 – 16].

2.4. *Radioactivation analyses of* ^{53}Mn

After the separation of ^{53}Mn with a Mn carrier, the chemical yield was determined by atomic absorption spectrometry or by flame photometry. The fraction was then dried on a pure Al foil and irradiated by thermal neutrons together with ^{53}Mn standard samples in the JRR 3 or JRR 2 reactor at the Japan Atomic Energy Research Institute, Tokai-mura, Japan. The Fe and Mn standard samples were also irradiated for the correction of small ^{54}Mn

contributions which were less than a few percent in all samples. The samples were stacked into a small volume of less than 1 cm^3 to minimize the effect of a possible flux gradient. This effect was found to be negligible in these irradiations.

Post-irradiation chemistry was performed in order to eliminate other gamma-activities. The ^{54}Mn in the sample was counted by a low-level 1.75″ well-type NaI counter with the anticoincidence setting or by a 100 cc Ge(Li) detector under heavy shielding. The precision was equal to or less than a few per cent [26].

3. Results

The contents of the cosmic-ray-produced nuclides are summarized in Table 1 for Grant and in Table 2 for Treysa. The mass spectrometric data and the assumptions for calculating the contents of the cosmic-ray-produced nuclides are described in the Appendix. The errors quoted are the combined errors of mass spectrometry and the chemical procedure. Errors of ^{53}Mn are obtained by quadratically adding the statistical errors in counting to uncertainties in recovery, but do not include the absolute error of the ^{53}Mn standard.

4. Discussion

4.1. Pre-atmospheric size of iron meteorites

It is possible to estimate the pre-atmospheric size of a meteorite by comparing the measured distributions of cosmic-ray-produced nuclides with calculated profiles. The depth profiles were calculated using a modified version [27] of the Kohman-Bender model [28] which is based on thick target bombardment data [20, 28].

The distribution of thick-target data were reproduced according to the diffusion-type equation of the Kohman-Bender model with the parameters presented in Table 3. This was integrated to obtain $\sigma(R, r)$, an effective cross section in a position, r, from the center in a spherical body with a radius R. The integration was made in a strict form rather than applying an approximation as described in the paper by Kohman-Bender [28]. The results, however, only raise the production by about 10% in the surface region.

The calculated profiles are shown in Figs. 4 and 5 normalized to the center. For comparison with the data, it is necessary to estimate the distance of each sample from the center of an original body. From noble gas data[4] and our results, we have estimated the position of the center of Grant to be around 125 mm left from the reference line shown in Figure 1. The determination of the pre-atmospheric center of Treysa is difficult because no rare gas data is available in the same plane as is used in the present investigation. The curve fitting of our data to the calculated patterns indicates the center to be around (0, +35) in Figure 2. The distances from these centers to each of our samples are given in Table 1 and 2. The experimental data are plotted against the distance from the center (Figs. 4 and 5) and compared with the calculated depth profiles of ^{40}K, ^{49}Ti and ^{53}Mn.

In Figs. 4 and 5 the profiles recently calculated by Yokoyama [29] are also given in dotted lines. His original data on chondrites are converted to iron meteorites by multiplying by a conversion factor taken as

$$1\text{ cm of iron meteorite} = \frac{\varrho_{Fe}}{\varrho_{chond.}} \cdot \frac{\lambda_{Fe}}{\lambda_{chond.}} \cong 1.8\text{ cm of chondrite}$$

(ϱ: density, λ: nuclear interaction mean free path). Our calculated profiles seem to agree well with Yokoyama's in objects with small R, but systematically deviate in objects with larger R. The experimental data on Grant and Treysa fitted very well to the calculated profile by Yokoyama. Deviation in our calculation from the experimental data for larger objects ($R \gtrsim 15$ cm) could be explained by underestimation of the secondary particles, that is, the thick target bombardment model experiments could have been performed with targets not applicable to the larger object.

The pre-atmospheric size of Grant and Treysa are estimated to be approximately 30 cm and 14 cm which corresponds to a mass of 880 kg and 90 kg respectively. The estimation for Grant agrees very well with 880 kg estimated by Fireman [5] and 750 kg by Maringer and Manning [30], but is considerably smaller than the estimation by Hoffman and Nier [4], who gave a pre-atmospheric mass of 2000 kg. For Treysa, Fechtig et al. [31] determined a pre-atmospheric radius to be $\cong$ 30 cm using rare gas data.

The estimation by our method should give a good approximation for the pre-atmospheric size unless

Table 1. Cosmic-ray-produced nuclides at various locations of the iron meteorite Grant[a].

Location	Distance from the center (mm)	Cosmic-ray-produced nuclides									k_2'
		^{40}K (10^{13} atoms/g)	^{43}Ca	^{46}Ti	^{47}Ti	^{49}Ti	^{50}Ti	^{50}V	^{54}Cr	^{53}Mn[b] (dpm/g)	
Q −260	235	0.545 ±0.011	1.6 ±0.2	2.95 ±0.07	3.59 ±0.05	5.71 ±0.11	0.24 ±0.02	—	21.2 ± 1.0	0.314 ±0.010	2.77
A −350	240	0.530 ±0.010	1.77 ±0.03	2.91 ±0.13	3.62 ±0.12	6.01 ±0.15	0.36 ±0.07	3.90 ±0.08	19.0 ± 0.8	0.366 ± 0.010	2.80
G −320	195	0.521 ±0.009	—	—	3.68 ±0.10	6.07 ±0.11	0.29 ± 0.04	4.11 ±0.14	—	0.368 ±0.011	2.91
E −240	150	0.471 ±0.007	—	2.74 ±0.06	3.49 ±0.04	5.78 ±0.10	0.23 ±0.02	3.77 ±0.06	21.3 ± 0.8	0.371 ±0.009	2.92
I −110	40	0.461 ±0.010	1.6 ±0.2	2.76 ±0.10	3.33 ±0.09	5.73 ±0.10	0.23 ±0.05	3.97 ±0.18	18.2 ± 0.9	0.373 ±0.010	2.90
G − 70	55	0.460 ±0.009	—	—	3.50 ±0.12	5.70 ±0.14	0.31 ±0.07	3.65 ±0.13	—	0.358 ±0.014	2.94
I − 55	80	0.460 ±0.011	1.46 ±0.09	2.69 ±0.33	3.51 ±0.09	5.73 ±0.15	0.25 ±0.13	3.68 ±0.15	17.1 ± 5.1	0.357 ±0.016	2.91
G − 15	110	0.496 ±0.011	—	—	3.54 ±0.11	5.75 ±0.14	0.26 ±0.03	—	—	0.374 ±0.016	2.93
G + 30	155	0.496 ±0.011	—	—	3.53 ±0.10	5.79 ±0.13	0.26 ±0.03	3.95 ±0.08	—	0.361 ±0.018	2.90
G + 60	185	0.490 ±0.012	—	—	3.51 ±0.11	5.93 ±0.13	0.27 ±0.05	—	—	0.360 ±0.016	2.88
K +100	245	0.512 ±0.009	—	2.71 ±0.08	3.38 ±0.06	5.39 ±0.09	0.24 ±0.01	3.34 ±0.11	—	0.319 ±0.009	2.78
F +150	275	0.510 ±0.009	—	—	3.43 ±0.08	5.44 ±0.12	0.26 ±0.03	3.30 ±0.11	—	0.304 ±0.015	2.65

[a] For cosmic-ray-produced nuclides of Ca and Cr other than ^{43}Ca and ^{54}Cr; see [14, 15, 17].

[b] Error for ^{53}Mn standard calibration is not included. For absolute values, ± 10% uncertainty in ^{53}Mn standard (Odessa-^{53}Mn standard) has to be added.

Table 2. Cosmic-ray-produced nuclides at various locations of the iron meteorite Treysa.

Location	Cosmic-ray-produced nuclides						k_2'
	^{40}K (10^{13} atoms/g)	^{47}Ti	^{49}Ti	^{50}Ti	^{50}V	^{53}Mn[a] (dpm/g)	
0, + 3	0.651 ±0.024	3.64 ±0.08	5.80 ±0.12	0.27 ±0.03	3.6 ±0.5	0.381 ±0.014	2.81
0, − 3	0.616 ±0.017	3.45 ±0.12	5.83 ±0.16	—	—	0.372 ±0.015	2.86
0, − 40	0.597 ±0.013	3.53 ±0.09	5.59 ±0.12	0.24 ±0.04	3.70 ±0.08	0.359 ±0.015	2.73
0, − 46	0.606 ±0.013	3.45 ±0.08	5.60 ±0.12	0.22 ±0.04	—	0.357 ±0.015	2.73
− 96, 0	0.607 ±0.022	3.42 ±0.09	5.29 ±0.14	—	3.61 ±0.33	0.322 ±0.013	2.60
−109, 0	0.604 ±0.013	3.38 ±0.07	5.15 ±0.11	0.23 ±0.06	3.4 ±0.8	0.299 ±0.012	2.56

[a] Error for ^{53}Mn standard calibration is not included. For absolute values, ± 10% uncertainties in ^{53}Mn standard (Odessa- I-^{53}Mn standard) have to be added.

Table 3. Selected parameters of the Kohman-Bender equation.

Particle parameters

Energy (BeV)	P_A (cm)	P_B (cm)	C_A (cm)	C_B (cm)	D_A (cm)	D_B (cm)
0.45	10	11.6	0.046	1.20	5.6	12.5
1.0	10	28	0.050	1.90	7.2	13.8
3.0	10	30	0.050	1.51	10.3	19.5
6.1	10	38	0.057	1.20	12.4	23

Nuclide parameters

Nuclides	Energy (BeV)	$\sigma_A(0)$ (mb)	$\sigma_B(0)$ (mb)	B_A (cm^{-1})	B_B (cm^{-1})
^{53}Mn	0.45	27	5.9	0.59	1.39
	1.0	40	13	0.59	0.75
	3.0	48	24	0.51	0.88
	6.1	57	39	0.57	0.69
^{49}Ti	0.45	22	1.6	0.37	0.82
	1.0	32	4.6	0.93	0.75
	3.0	46	12	0.57	1.00
	6.1	46	20	0.74	0.76
^{40}K	0.45	2.5	0.063	0.11	0.26
	1.0	8.2	0.53	0.29	0.44
	3.0	16	2.2	0.33	0.54
	6.1	16	4.6	0.30	0.40

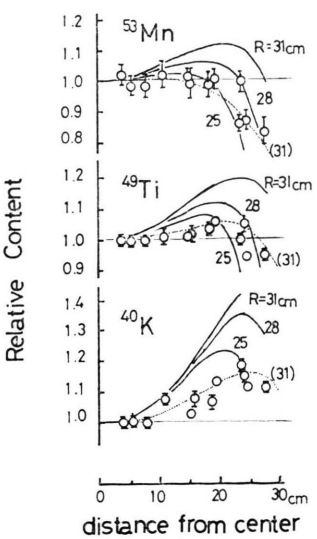

Fig. 4. Radial distributions of cosmic-ray-produced ^{53}Mn, ^{49}Ti and ^{40}K in the iron meteorite Grant. Calculated distributions of these nuclides for spherical iron meteoroids of various size are also shown in relative numbers. Dotted lines show the profiles for $R = 31$ cm of iron meteoroid taken from the calculation on chondrites by Yokoyama [29]. (^{40}K profiles was extraporated from ^{44}Ti.)

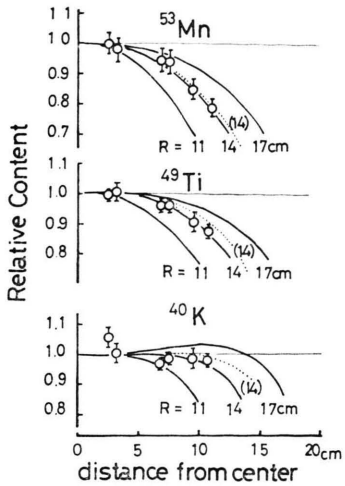

Fig. 5. Radial distributions of cosmic-ray-produced ^{53}Mn, ^{49}Ti and ^{40}K in the iron meteorite Treysa. Calculated distributions of these nuclides for spherical iron meteoroids of various size are also shown in relative numbers. Dotted lines show the profiles for $R = 14$ cm of iron meteoroid taken from the calculation on chondrites by Yokoyama [29]. (^{40}K profiles was extraporated from ^{44}Ti).

the meteorite was actually quite elongated or irregularly shaped.

4.2. *On the space erosion of iron meteorites*

Exposure ages of iron meteorites are generally larger than those of stone meteorites and are mostly distributed in the range $10^8 - 10^9$ years. One of explanations for this fact is a space erosion model proposed by Whipple and Fireman [32]. The distribution pattern of spallogenic stable nuclides should change with time if space erosion has a considerable effect on iron meteorites. However, radioactive spallogenic nuclides reflect only recent irradiation conditions and are not so influenced by space erosion as stable isotopes.

The total production $Q(R_0, r)$ per unit volume at the distance r from the center of a spherical meteoroid with the last pre-atmospheric radius R_0 during the exposure time can be calculated for various values of R_0 as follows:

$$Q(R_0, r) = \int_{R_0}^{R_0+\delta} \int_{E_0}^{\infty} n\,\sigma(R, r, E) \frac{1}{(-\mathrm{d}R/\mathrm{d}t)} J(E)\,\mathrm{d}E\,\mathrm{d}R \tag{1}$$

with $J(E)\,\mathrm{d}E$, the fraction of cosmic ray flux with an energy between E and $E + \mathrm{d}E$; E_0 the threshold

energy; n, the number of target atoms per unit volume and δ, the extent of erosion defined as $\int_{-T}^{0} (dR/dt)\,dt$, ($T$: exposure age). The spectrum and intensity of cosmic rays is assumed to have been constant throughout the exposure history of the meteorite. When erosion has occurred continuously, Eq. (1) becomes

$$Q(R_0, r) = \frac{1}{e} \int_{R_0}^{R_0+eT} n\,\bar{\sigma}_c(R, r)\,J\,dR \qquad (2)$$

where e is the errosion rate, $\bar{\sigma}$ is mean cross section for cosmic ray spectrum and J is the cosmic ray flux. The distribution pattern corresponding to various erosion rates can be numerically calculated from the $\bar{\sigma}$ calculated for different R and r. Calculations were made for the ^{49}Ti isotope based on the production profiles given by Yokoyama [29] since they agree quite well with the experimental data for each nuclide. Figure 6 shows calculated ^{49}Ti distributions which experienced the continuous erosion corresponding to $e = 0$ and 0.8 Å/y, for $R_0 = 30$ cm (a) and for $R_0 = 14$ cm (b). Figure 6 shows that erosion was not significant for Grant and Treysa and less than ~ 5 cm during the period of exposure. The upper limit of erosion rate for iron meteorites is calculated to be 0.8 Å/y. McDonnel and Ashworth [33] have estimated the erosion effects on meteorites based on the calculation of ion-sputtering and hypervelocity impacts. They obtain erosion for metallic objects with masses of 10^2 to 10^3 kg of $\sim 1 \times 10^{-8}$ cm/y. The upper limit obtained for Grant and Treysa is only slightly lower than their estimate.

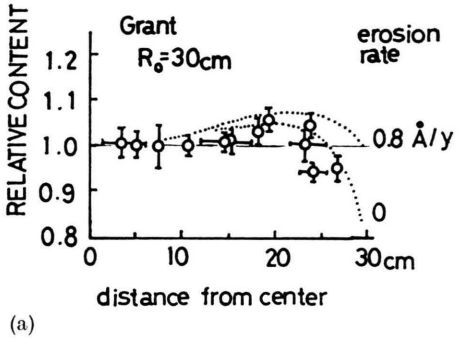

(a)

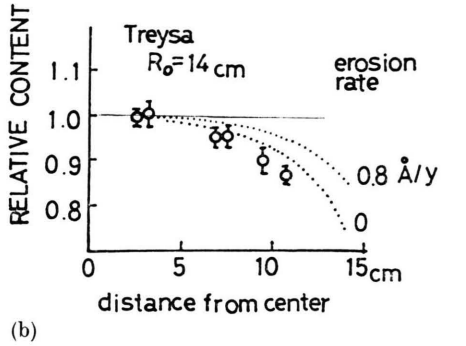

(b)

Fig. 6. Continuous erosion model for ^{49}Ti distribution in Grant, (a), and Treysa, (b). Observed ^{49}Ti profiles were compared with the calculated profiles expected in the case that continuous erosion of 0.8 Å/y had occured during the exposure time of Grant (T = 695 my) and Treysa (T = 625 my). Calculation was made based on the profiles given by Yokoyama [29], R_0's were sestimated from ^{53}Mn data.

The consequence of the low erosion rate obtained here may be discussed in connection with the interpretation of exposure ages. The maximum effects for a Grant-sized meteoroid were calculated to give ages only $\sim 8\%$ and $\sim 3\%$ lower (^{36}Cl-^{36}Ar and ^{53}Cr-^{53}Mn exposure ages, respectively), than the real exposure ages, which we may take as the ^{40}K-^{41}K age, if cosmic-ray intensity has been nearly constant. Therefore the large ($\sim 30\%$) differences between ^{36}Cl-^{36}Ar and ^{40}K-^{41}K ages [34] cannnot be explained by space erosion alone.

4.3. Depth Dependence of Spallation Systematics

One of the goals in understanding the interaction between cosmic rays and meteorites is the determination of the pre-atmospheric size of the meteorite and the location of specific samples within this meteorite. For this reason it is very useful to study the depth effect of spallogenic nuclides. Geiss et al. [35] and Stauffer and Honda [13] analysed the cosmic-ray products in iron meteorites in view of the spallation systematics which can be described by the empirical equation,

$$C(A) = k_1 (\Delta A)^{-k_2} \qquad (3)$$

where $C(A)$ is the spallogenic concentration of the isobar A, $\Delta A = 56 - A$, with $A \leqq 50$, k_1 is constant and k_2 is depth-dependent parameter [20, 35], i. e. energy dependent with a smaller value for the higher energy. Taking all available data for spallogenic nuclides in Grant, a better fit to the data is given by

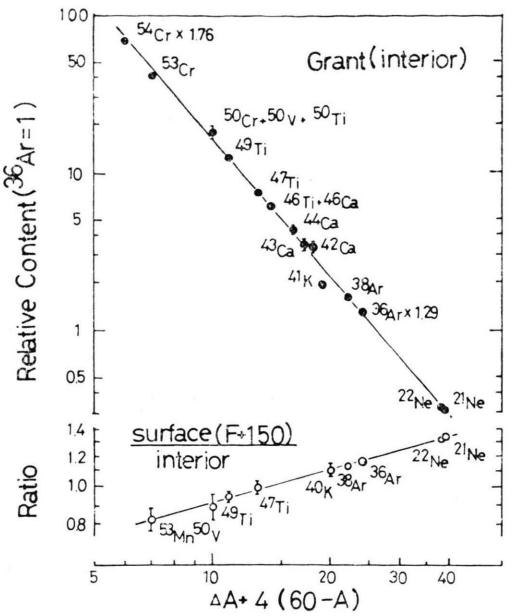

Fig. 7. Relationship between the total isobaric yield and mass number plotted as $\ln C$ vs. $\ln(\Delta A+\alpha)$, where $\Delta A = 56 - A$ and $\alpha = 4$. Figure (upper) shows for the interior samples of Grant (G-70 and I-110). The ratio of the contents in surface sample (F + 150) to the interior sample is also shown in the figure (lower).

Eq. (3′),

$$C(A) = k_1'(\Delta A+\alpha)^{-k_2'} \qquad (3')$$

with $\alpha = \text{constant}(\cong 4)$, as illustrated in Fig. 7 for the interior sample (average for Grant I-55 and G-70). The relative contents (ratios of surface/interior) in the surface sample (F + 150) are also shown as a function of $(\Delta A+\alpha)$. The parameters k_2' are listed in the last column of Tables 1 and 2. The increase of k_2' is very gradual from the surface to the center except in the top surface layer where k_2' is a rather steep function of depth.

The production of mass 41 is significantly lower than expected from the line of Figure 7. The $^{41}K_{sp.}$ was calculated from the ^{40}K data multiplied by $(^{41}K/^{40}K)_{sp.} = 1.952$ which is calculated from the Grant data of Voshage [34]. A deficit of about 20% of ^{41}K in Grant is probably due to the closed shell effect at proton number 20 and neutron number 20. The production of $A = 41$ is supposed to be suppressed by unfavorable proton evaporation from the excited ^{42}Ca nuclei and proton decay of excited ^{41}Sc.

These observations suggest that the spallation systematics as described by Eq. (3′) possibly breaks down to some extent around the mass region of K isotopes where products with proton and neutron magic numbers are involved in the reaction.

4.4. *Cosmic-Ray-Exposure Age and Constancy of Cosmic-Ray Intensity*

Exposure ages have been frequently discussed in relation to the secular variation of the galactic cosmic-ray intensity. Tanaka and Inoue [36] have recently measured ^{10}Be depth profile in several deep-sea sediment cores and concluded that the galactic cosmic-ray intensity has been constant within ±30% in the last 2.5 million years. However it has been suggested that there was a variation of the cosmic-ray intensity on a time scale of 10^8 years, on the basis of a significant difference between exposure age calculated by the ^{40}K-^{41}K method and other methods [37 – 39]. For this reason, ^{53}Cr-^{53}Mn is another pair of spallogenic nuclides which provides additional information on the cosmic-ray-variation.

The apparent exposure age, T, can be calculated from Eq. (4),

$$T = \frac{\gamma_a C_s}{\gamma_s C_a} \qquad (4)$$

where the suffix "a" is refered to a radioactive isobar, "s" to a stable isobar to which the radioactivity decays, C to the content of the product in atoms/g for the stable isobar and in disintegration per year/g for the radioactive isobar and γ is the fraction of production among the isobars. Charge distribution in the production of isobars produced by cosmic-rays have been discussed in our previous paper [17]. It was found that γ could be well expressed in the semiempirical forms as proposed by Rudstam [40].

$$\gamma(A,Z) = \sqrt{R/\pi}\exp[-R(Z-SA)^2] \qquad (5)$$

with $R = 1.4 \pm 0.15$ and $S = 0.470 \pm 0.001$. A is the mass number and Z is the atomic number.

Table 4 shows the calculated ^{53}Cr-^{53}Mn exposure ages for several locations on Grant. The $\gamma(^{53}Mn)$ was calculated as 0.79 according to Eq. (5), which is in good agreement with 0.79 ± 0.04, computed from the experimental data of 600 GeV p-spallation by Perron [41] and 0.81 from the Monte Carlo calculation in thick target bombardments with 1-

Table 4. ^{53}Cr-^{53}Mn exposure age of Grant calculated for several sample locations.

Sample location	Distance from the center (mm)	^{53}Cr [a] (10^{13} atoms/g)	^{53}Mn-^{53}Cr exposure age [b] (10^8 y)
A-350	240	21.1 ± 1.7	8.3 ± 1.1
Q-260	235	21.5 ± 1.9	9.9 ± 1.4
E-240	150	21.4 ± 1.0	8.3 ± 1.0
I-55	80	21.3 ± 9.4	8.6 ± 3.9
I-110	40	19.0 ± 1.3	7.4 ± 0.9

[a] Shima et al. [14].

[b] $\gamma(^{53}Mn) = 0.79$ was used. The decay of ^{53}Mn due to possible long terrestrial age (τ) of the meteorite is corrected assuming $\tau = 1.7 \pm 0.8 \times 10^5$ y. These values are compared to the ^{41}K-^{40}K age, 6.95×10^8 y [34].

and 3-BeV protons by Armstrong [42]. The agreement with p-spallation data, however, could be fortuitous, because the application of Eq. (5) to a product near the target nuclide may not be appropriate and the relative production of ^{53}Cr is expected to be higher in meteorites than in p-spallation reactions, due to the contribution of $^{56}Fe(n, \alpha)^{53}Cr$. The ages given in Table 4 are corrected for a long terrestrial age of Grant, which was estimated to be $(1.7 \pm 0.8) \times 10^5$ years from $^{36}Cl/^{10}Be$ ratio [21]. A higher value of the exposure age in sample Q-260 may indicate a break down of the edges of the meteorite in relatively recent history. The ages obtained are slightly longer than the ^{40}K-^{41}K age, which could indicate a lower cosmic-ray intensity about 10^7 years ago compared to the present-day intensity.

The above effect, however, might also be explained by the use of a too large $\gamma(^{53}Mn)$. In order to confirm the existence of secular cosmic-ray variations it is necessary to obtain the $\gamma(^{53}Mn)$ value experimentally from a study of the n-spallation reaction.

Acknowledgement

The authors are indebted to the following individuals for providing us with meteorite samples: Dr. K. Fredriksson, Smithsonian Institution, U.S. National Museum, Washington, D.C. (USA), Professor J. R. Arnold, University of California, San Diego, California, (USA), Dr. E. P. Henderson, Smithsonian Institution, U.S. National Museum, Washington, D.C. (USA) and Professor H. Wänke, Max-Planck-Institut für Chemie, Mainz (Germany).

Appendix

The Tables A. 1, A. 2 and A. 3 show the mass spectrometric data of K, Ti and V in Grant and Treysa. The measured isotopic ratios of reagents K, Ti and V and of spikes used are also given in the tables.

Errors quoted with the data of cosmic-ray-produced nuclides include ambiguities introduced from the chemical procedures which were estimated as 2% for each value, besides the statistical error of the mass spectrometry.

For the estimation of spallogenic isotopic ratios of K the following assumptions were made:

$$(39)_c/(40)_c = 1.4\,,$$

$$(41)_c/(40)_c = 1.8\,.$$

The ratio, 1.8, is somewhat higher than experimental values obtained from the data without spike given in the bottom of Table A. 1 and also by Voshage [34]. Because of the predominant amount of spallogenic ^{40}K in the measured ^{40}K, the effect of a small difference in this ratio is not significant for the results.

The spallogenic ^{48}Ti, $(48)_c$, was assumed to be $\sqrt{(47)_c \cdot (49)_c}$. Since the cosmic-ray-induced fraction was dominant in the measured Ti isotopic ratios, the results are not strongly affected by this assumption. In the spiked sample $(46)_c/(48)_c = 0.63$, obtained from the mean values of non-spiked samples, was used for the calculation.

For V most of the measured V isotopic ratio $(51)_m/(50)_m$ ranged between 4 and 10 in non-spiked samples. The estimated ratio of the cosmogenic V isotopic ratio was 3, thus the laboratory contamination should have been less than 20×10^{-9} g. For the calculation of the cosmic-ray-produced ^{50}V, the estimated contamination of $(12 \pm 8) \times 10^{-9}$ g was taken into account.

Table A.1. Details of the data for obtaining cosmogenic ^{40}K.

Sample location	Sample taken (g)	Spike added (μg)	K found (ppm)	K peak height ratio 39/41	K peak height ratio 40/41	Cosmogenic ^{40}K (10^{13}atoms/g)
			Grant			
Q −260	0.885	7.11	0.83	148.32 ± 0.48	0.009406 ± 0.000028	0.545 ± 0.011
A −350	1.251	17.67	0.51	367.36 ± 1.83	0.01487 ± 0.00009	0.525 ± 0.011
	1.088	25.68	2.03	174.96 ± 0.58	0.006226 ± 0.000019	0.541 ± 0.012
	0.779	5.17	0.59	168.55 ± 0.36	0.01165 ± 0.00042	0.522 ± 0.030
					mean	0.530 ± 0.010
G −320	1.055	9.33	0.227	475.24 ± 4.52	0.02547 ± 0.00060	0.523 ± 0.019
	1.048	0.287	0.120	44.369 ± 0.105	0.04088 ± 0.00020	0.520 ± 0.011
					mean	0.521 ± 0.009
E −240	1.773	12.47	0.98	115.56 ± 0.37	0.007508 ± 0.000021	0.474 ± 0.010
	1.155	7.04	0.262	312.66 ± 1.11	0.01987 ± 0.00055	0.447 ± 0.020
	0.914	0.274	0.613	20.852 ± 0.081	0.009412 ± 0.000115	0.490 ± 0.012
	1.252	5.96	1.70	54.666 ± 0.225	0.004898 ± 0.000042	0.474 ± 0.012
	1.085	9.24	0.250	429.62 ± 3.07	0.02127 ± 0.00066	0.445 ± 0.022
					mean	0.471 ± 0.007
I −110	1.018	7.31	3.06	48.181 ± 0.133	0.003547 ± 0.000152	0.443 ± 0.050
	0.963	8.51	0.61	211.58 ± 0.69	0.01107 ± 0.00012	0.465 ± 0.012
					mean	0.461 ± 0.010
G − 70	0.794	5.19	0.210	396.49 ± 1.46	0.02423 ± 0.00007	0.460 ± 0.009
I − 55	1.784	31.83	0.471	471.95 ± 1.80	0.01538 ± 0.00010	0.460 ± 0.011
G − 15	1.090	6.35	0.296	271.06 ± 1.34	0.01931 ± 0.00014	0.496 ± 0.011
G + 30	0.850	4.86	0.145	474.57 ± 2.58	0.03372 ± 0.00027	0.496 ± 0.011
G + 60	0.644	4.50	0.212	415.11 ± 2.13	0.02527 ± 0.00026	0.490 ± 0.012
K +100	1.239	9.78	0.107	754.03 ± 6.22	0.04159 ± 0.00077	0.495 ± 0.015
	0.964	4.40	0.389	174.16 ± 0.96	0.01609 ± 0.00016	0.537 ± 0.012
	0.793	0.253	1.44	17.067 ± 0.041	0.005125 ± 0.000035	0.505 ± 0.011
					mean	0.512 ± 0.009
F +150	0.952	5.48	0.188	388.46 ± 4.02	0.02865 ± 0.00022	0.521 ± 0.012
	0.952	5.48	0.177	407.90 ± 2.15	0.02912 ± 0.00035	0.500 ± 0.012
					mean	0.510 ± 0.009
			Treysa			
0, + 3	1.083	0.264	0.40	22.323 ± 0.083	0.01710 ± 0.00048	0.651 ± 0.024
0, − 3	0.904	0.308	1.02	18.645 ± 0.210	0.007546 ± 0.000140	0.616 ± 0.017
0, −40	0.899	0.213	0.61	19.354 ± 0.167	0.01111 ± 0.00011	0.597 ± 0.013
0, −46	0.937	0.392	0.67	22.798 ± 0.169	0.01042 ± 0.00009	0.606 ± 0.013
− 96, 0	0.791	0.329	0.52	25.248 ± 0.280	0.01290 ± 0.00037	0.607 ± 0.022
−109, 0	0.934	0.240	0.78	18.517 ± 0.094	0.009132 ± 0.000041	0.604 ± 0.013
Reagent (mean of 16 runs Sept. 1967—April 1970)				13.877 ± 0.045	0.001722 ± 0.000009	
Spike (mean of 2 runs)				2668.4 ± 13.3	0.03641 ± 0.00018	
						cosmogenic 41/40
			Grant			
G −320	1.0	—	0.19	13.494 ± 0.084	0.02851 ± 0.00022	1.1 ± 0.4
I −110	1.4	—	0.47	13.786 ± 0.041	0.01138 ± 0.00003	0.8 ± 0.4
	1.0	—	0.37	13.466 ± 0.068	0.01371 ± 0.00006	2.6 ± 0.5
					mean	2.0 ± 0.5
I − 55	1.3	—	0.22	13.516 ± 0.039	0.02211 ± 0.00008	1.4 ± 0.2
K +100	1.1	—	0.25	13.513 ± 0.040	0.02174 ± 0.00020	1.4 ± 0.2

Table A.2. Details of the data for obtaining cosmogenic titanium isotopes.

Sample location	Sample taken (g)	Spike added (μg)	Ti found (ppm)	Ti peak height ratio × 100			
				46/48	47/48	49/48	50/48
				Grant			
Q −260	1.113	0.207	0.15	136.99 ± 1.07	14.47 ± 0.15	11.087 ± 0.094	—
	0.885	0.0497	0.38	28.37 ± 0.45	11.15 ± 0.13	8.97 ± 0.15	—
A −350	1.251	0.124	0.11	113.25 ± 1.57	14.98 ± 0.19	13.00 ± 0.08	—
	0.779	0.0361	1.4	14.833 ± 0.095	10.212 ± 0.067	7.897 ± 0.052	7.306 ± 0.114
G −320	1.055	0.0677	0.055	146.63 ± 1.04	18.760 ± 0.172	18.640 ± 0.124	7.579 ± 0.069
	1.048	0.0652	0.049	160.76 ± 3.30	19.521 ± 0.684	20.167 ± 0.419	—
E −240	0.858	0.210	0.13	187.7 ± 1.8	15.56 ± 0.12	11.56 ± 0.09	7.765 ± 0.082
	1.773	0.0871	0.06	114.2 ± 3.0	17.88 ± 0.52	17.80 ± 0.56	7.52 ± 0.23
	1.252	0.0520	0.038	148.62 ± 2.12	21.292 ± 0.266	23.554 ± 0.230	7.496 ± 0.063
	1.085	0.0704	0.041	191.09 ± 1.15	21.031 ± 0.114	21.472 ± 0.140	7.629 ± 0.056
I −110	1.018	0.0511	0.14	55.43 ± 0.67	12.86 ± 0.18	11.78 ± 0.24	7.10 ± 0.17
	0.963	0.0594	0.074	108.76 ± 0.52	16.078 ± 0.076	15.433 ± 0.122	7.511 ± 0.060
G − 70	0.794	0.0453	0.059	125.55 ± 1.28	17.680 ± 0.165	17.390 ± 0.132	7.587 ± 0.125
I − 55	1.784	0.222	0.085	163.35 ± 1.01	16.397 ± 0.121	13.853 ± 0.098	7.60 ± 0.57
G − 15	1.090	0.0555	0.068	101.93 ± 0.77	16.636 ± 0.139	16.297 ± 0.116	7.424 ± 0.050
G + 30	0.850	0.0425	0.062	109.60 ± 0.40	17.275 ± 0.114	17.268 ± 0.095	7.436 ± 0.047
G + 60	0.644	0.0393	0.079	102.66 ± 0.59	15.857 ± 0.104	15.203 ± 0.082	7.458 ± 0.058
K +100	1.239	0.0744	0.050	151.70 ± 0.84	18.970 ± 0.108	18.570 ± 0.096	7.581 ± 0.037
	0.964	0.0385	0.087	67.66 ± 0.51	14.805 ± 0.132	13.904 ± 0.158	7.333 ± 0.096
F +150	0.952	0.0479	0.069	99.15 ± 0.31	16.356 ± 0.073	15.675 ± 0.068	7.444 ± 0.039
				Treysa			
0, + 3	1.083	0.0600	0.044	163.50 ± 0.72	20.750 ± 0.092	21.262 ± 0.072	7.581 ± 0.064
0, − 3	0.904	0.0700	0.066	143.29 ± 0.79	17.250 ± 0.147	16.312 ± 0.168	—
0, −40	0.899	0.0483	0.047	146.33 ± 0.99	19.531 ± 0.128	19.628 ± 0.114	7.494 ± 0.080
0, −46	0.937	0.0891	0.061	177.36 ± 0.51	18.019 ± 0.051	16.237 ± 0.076	7.624 ± 0.051
96, 0	0.791	0.0748	0.069	157.47 ± 0.88	17.060 ± 0.073	14.809 ± 0.138	—
109, 0	0.934	0.0545	0.062	120.70 ± 0.41	17.095 ± 0.037	15.894 ± 0.043	7.479 ± 0.101
Reagent (mean of 11 runs Aug. 1967—Oct. 1969)				10.871 ± 0.022	9.949 ± 0.015	7.427 ± 0.011	7.233 ± 0.015
Spike (mean of 2 runs)				732.6 ± 2.4	24.37 ± 0.12	9.17 ± 0.05	9.69 ± 0.10
				Grant			
Q −260	1.0	—	0.21	12.071 ± 0.075	11.579 ± 0.047	10.269 ± 0.051	7.245 ± 0.035
	1.5	—	0.026	26.537 ± 0.191	29.647 ± 0.171	41.234 ± 0.359	6.584 ± 0.031
A −350	1.0	—	0.17	12.466 ± 0.077	11.986 ± 0.078	11.107 ± 0.076	7.260 ± 0.042
	1.09	—	0.07	14.91 ± 0.25	15.14 ± 0.75	17.47 ± 0.73	6.52 ± 0.54
E −240	1.7	—	0.17	12.33 ± 0.12	11.97 ± 0.06	11.03 ± 0.08	7.156 ± 0.063
	3	—	0.25	11.885 ± 0.048	11.325 ± 0.040	9.902 ± 0.044	7.208 ± 0.035
	1.3	—	0.046	17.659 ± 0.147	18.968 ± 0.148	23.657 ± 0.152	6.993 ± 0.047
I −110	1.4	—	0.12	13.18 ± 0.09	12.83 ± 0.09	12.76 ± 0.11	7.048 ± 0.068
	1.0	—	0.14	12.50 ± 0.27	12.18 ± 0.20	11.56 ± 0.22	7.13 ± 0.019
I − 55	2.05	—	0.12	12.77 ± 0.24	12.73 ± 0.34	12.60 ± 0.27	7.06 ± 0.20
	1.3	—	0.04	19.5 ± 1.5	21.3 ± 1.5	26.5 ± 1.8	7.37 ± 0.64
K +100	1.1	—	0.037	19.623 ± 0.139	21.273 ± 0.141	27.169 ± 0.243	6.933 ± 0.065

Table A.3. Details of the data for obtaining cosmogenic ^{50}V.

Sample location	Sample taken (g)	Spike added (μg)	V peak height ratio 51/50	Correction ^{50}Ti (%)	Correction ^{50}Cr (%)	Cosmogenic ^{50}V (10^{13} atoms/g)
			Grant			
A −350	1.251	0.497	96.4 ± 1.9	15	12	3.90 ± 0.08
G −320	1.048	1.239	185.9 ± 2.7	30	7	4.11 ± 0.14
E −240	1.252	0.352	76.1 ± 4.9	20	65	3.80 ± 0.30
	1.085	0.283	72.7 ± 1.3	7	15	3.76 ± 0.11
					mean	3.77 ± 0.11
I −110	1.018	0.206	57.4 ± 2.0	24	7	3.97 ± 0.18
G − 70	0.794	0.307	100.2 ± 2.2	50	15	3.65 ± 0.13
I − 55	1.784	0.898	118. ± 3	25	25	3.68 ± 0.15
G + 30	0.850	0.287	85.5 ± 0.7	10	10	3.95 ± 0.08
K +100	1.239	0.300	74.7 ± 2.6	5	55	3.37 ± 0.16
	0.793	1.095	222.9 ± 5.9	70	30	3.30 ± 0.21
					mean	3.34 ± 0.11
F +150	0.952	0.324	98.0 ± 2.0	60	20	3.30 ± 0.11
			Treysa			
0, + 3	1.083	1.141	189 ± 15	300	250	3.6 ± 0.5
0, −40	0.899	0.918	182.2 ± 1.0	13	1	3.70 ± 0.08
− 96, 0	0.791	1.423	239.6 ± 8.7	200	15	3.61 ± 0.33
−109, 0	0.934	1.036	198 ± 24	40	200	3.4 ± 0.8
Reagent (mean of 7 runs, Oct. 1967—April 1969)			399.0 ± 1.9			
			Grant			
Q −260	1.5	—	4.29 ± 0.23	3	70	
A −350	1.0	—	9.80 ± 0.20	3	44	
	1.09	—	5.03 ± 0.18	41	23	
E −240	1.3	—	7.33 ± 0.21	5	50	
I −110	1.0	—	8.63 ± 0.30	8	27	
I − 55	1.3	—	5.00 ± 0.15	22	3	
K +100	1.1	—	8.31 ± 0.33	2	100	

[1] F. A. Paneth, P. Reasbeck, and K. I. Mayne, Geochim. Cosmochim. Acta **2**, 300 (1952).
[2] F. A. Paneth, P. Reasbeck, and K. I. Mayne, Nature London **172**, 200 (1953).
[3] A. P. Vinogradov, I. K. Zadorozhnyi, and K. P. Frorenskii, Geokhimiya **6**, 443 (1957).
[4] J. H. Hoffman and A. O. Nier, Phys. Rev. **112**, 2112 (1958).
[5] E. L. Fireman, Nature London **181**, 1725 (1958).
[6] H. Wänke and H. Hintenberger, Z. Naturforsch. **13a**, 895 (1958).
[7] E. L. Fireman, Planet. Space Sci. **1**, 66 (1959).
[8] J. H. Hoffman and A. O. Nier, Geochim. Cosmochim. Acta **17**, 32 (1959).
[9] P. Signer and A. O. Nier, J. Geophys. Res. **65**, 2947 (1960).
[10] J. H. Hoffman and A. O. Nier, J. Geophys. Res. **65**, 1063 (1960).
[11] R. J. Wright, L. A. Simms, M. A. Reynolds, and D. D. Bogard, J. Geophys. Res. **78**, 1308 (1973).
[12] L. Schultz and P. Signer, Earth Plunet. Sci. Lett. **30**, 191 (1976).
[13] H. Stauffer and M. Honda, J. Geophys. Res. **66**, 3584 (1961); ibid **67**, 3503 (1962).
[14] Masako Shima and M. Honda, Earth Planet. Sci. Lett. **1**, 65 (1966); Shitsuryo Bunseki (Mass Spectroscopy) **14**, 23 (1966).
[15] Masako Shima, M. Imamura and M. Honda, Shitsuryo, Bunseki (Mass Spectroscopy) **16**, 277 (1968).
[16] M. Imamura, Masako Shima, and M. Honda, Shitsuryo Bunseki (Mass Spectroscopy) **16**, 291 (1968).
[17] Masako Shima, M. Imamura, H. Matsuda, and M. Honda, in: Meteorite Research (Ed. P. M. Millman), D. Reidel. Netherlands, 1969, p. 335.
[18] M. Imamura, Masako Shima, and M. Honda, in: Recent Developments in Mass Spectroscopy. (Eds. K. Ogata and T. Hayakawa), Univ. Park Press, Baltimore 1970, p. 647.
[19] K. Imamura, Masako Shima, and M. Honda, Earth Planet. Sci. Lett. **26**, 56 (1975).
[20] M. Honda, J. Geophys. Res. **67**, 4847 (1962).
[21] M. Honda and J. R. Arnold, Science **143**, 203 (1964
[22] M. Honda and M. Imamura, Phys. Rev. C **4**, 1182 (1971).

[23] R. D. Beckinsale and N. H. Gale, Earth Planet. Sci. Lett. **6**, 289 (1969).
]24] Chart of Nuclides 12th ed. (1977).
[25] H. Irving and J. J. Cox, Analyst **83**, 526 (1958).
[26] M. Imamura, H. Matsuda, K. Horie, and M. Honda, Earth Planet. Sci. Lett. **6**, 165 (1969).
[27] M. Imamura, Thesis (Dr. of Science), The Univ. Tokyo, 1970.
[28] T. P. Kohman and M. L. Bender, in: High Energy Reactions in Astrophysics (Ed. B. S. P. Shen), W.A. Benjamin, New York 1967, p. 169.
[29] Y. Yokoyama, private communication.
[30] R. E. Maringer and G. K. Manning, Geochim. Cosmochim. Acta **18**, 157 (1960).
[31] H. Fechtig, W. Gentner, G. Kistner, Geochim. Cosmochim. Acta **18**, 72 (1960).
[32] F. L. Whipple and E. L. Fireman, Nature London **183**, 1315 (1959).
[33] J. A. M. McDonnel and D. G. Ashworth, Space Research XII. Akademie-Verlag, Berlin **1972**, p. 332.
[34] H. Voshage, Z. Naturforsch. **22a**, 477 (1967).
[35] J. Geiss, H. Oeschger, and U. Schwarz, Space Sci. Rev. **1**, 197 (1962).
[36] S. Tanaka and T. Inoue, Earth Planet. Sci. Lett. **45**, 181 (1979).
[37] H. Voshage, Z. Naturforsch. **17a**, 422 (1962).
[38] O. A. Schaffer and D. Heymann, J. Geophys. Res. **70**, 215 (1965).
[39] W. Hampel and O. A. Scheaffer, Earth Planet. Sci. Lett. **42**, 348 (1978).
[40] G. Rudstam, PhD Thesis, Uppsala 1956.
[41] C. Perron, Phys. Rev. **C 14**, 1108 (1976).
[42] T. W. Armstrong, J. Geophys. Res. **74**, 1361 (1969).